

## Proton-neutron mass difference, electroproduction, and photoabsorption in an analytic model of the virtual Compton amplitude

B. B. Deo\* and B. P. Mahapatra

Department of Physics, Utkal University, Bhubaneswar-751004, Orissa, India

(Received 16 January 1975)

An analytic model of the forward (virtual) Compton amplitude is proposed which satisfies  $\nu$  plane analyticity,  $s-u$  crossing symmetry, Regge behavior, and Bjorken scale invariance in appropriate limits. The model is constructed using the method of conformal mapping. Very good fits are obtained to the electroproduction data on  $\nu W_2^p$ ,  $2mW_1^p$ ,  $\nu W_2^p - \nu W_2^n$ ,  $\nu W_2^n / \nu W_2^p$ ,  $\nu R_p$ , and  $1 + \nu W_2^n / \nu W_2^p$ , and to the photoabsorption data on  $\sigma_T(\gamma p)$ ,  $\sigma_T(\gamma n)$ , and  $\sigma_T(\gamma p) - \sigma_T(\gamma n)$ . The scale-invariance breaking at finite  $Q^2$  as exhibited by the data on  $\nu W_2^p$  plotted as a function of  $Q^2$  with  $\omega$  fixed is also successfully reproduced. The  $p-n$  mass difference calculated using the Cottingham formula is finite. In particular, it is shown that a set of parameters exists for which the general condition for no logarithmic divergence even in the presence of Bjorken scaling given by  $\lim_{Q^2 \rightarrow \infty} Q^4 \Delta t_1^f(-Q^2, 0) = (\alpha m / \pi) \int_0^1 dx [\Delta F_2(x) + 2x \Delta F_1(x)]$  can be realized consistent with theoretical consideration and experimental data. The final result of our calculation of the mass difference is  $(-1.96 \pm 0.52)$  MeV, which is to be compared with the experimental value of  $-1.293$  MeV.

### I. INTRODUCTION

The problem of  $p-n$  mass difference, which is probably the oldest puzzle in hadron physics, has remained unsolved in spite of numerous attempts<sup>1</sup> in the past two decades. The earliest attempt can be traced back to Feynman and Speisman,<sup>2</sup> who conjectured that in the Born approximation the negative magnetic energy may supersede the positive Coulomb contribution at sufficiently high photon momentum, leading to a correct value of the mass difference. This conjecture has proved inadequate for the nucleon as both electric and magnetic form factors fall off very fast. The "notorious" wrong sign<sup>3</sup> of the Born contribution to the  $p-n$  mass difference provided motivation to include further strong-interaction effects in the calculation. This was made feasible by the important work of Cottingham<sup>4</sup> which related the electromagnetic self-mass  $\delta m$ , of a hadron to the forward amplitude of Compton scattering of virtual photons off the hadron. By a Wick rotation in the photon-energy plane  $\delta m$  was further related to the experimentally accessible deep-inelastic structure functions describing the electron-hadron scattering. Harari<sup>5(a)</sup> showed from consideration of Regge-pole exchanges in the crossed channel that the  $\Delta I=2$  mass differences are adequately described by the Born term alone (thus explaining the successful calculations of  $\pi^+ - \pi^0$  and  $\Sigma^+ - \Sigma^- - 2\Sigma^0$  mass differences<sup>2,5(b)</sup>), while  $\Delta I=1$  mass differences (such as the  $p-n$  or  $K^+ - K^0$ ) could have additional contributions from the subtraction term in the invariant Compton amplitude  $t_1(\nu, q^2)$ .

The evaluation of this unknown subtraction term

in determining its contribution to  $\Delta I=1$  mass differences presented one of the major difficulties. With the advent of "scaling" of the deep-inelastic structure functions, i.e.,  $W_1(\nu, Q^2)$  and  $\nu W_2(\nu, Q^2)$  becoming functions of a single dimensionless variable  $\omega = 2m\nu/Q^2$  in the Bjorken-scaling limit<sup>6</sup> ( $Q^2 \rightarrow \infty$ , with  $\omega$  fixed), it was discovered<sup>7</sup> that the em self-mass  $\delta m$  diverges logarithmically unless some apparently unlikely cancellations occur among terms in the Cottingham formula for the self-mass. Moffat and Wright<sup>8</sup> examined the conditions which would lead to a finite  $p-n$  mass difference  $\Delta m$  even if the self-masses were individually divergent. They showed that it would be possible to obtain a finite mass difference  $\Delta m$ , provided that the differences  $\nu W_2^p - \nu W_2^n$  and  $W_1^p - W_1^n$  do not have nontrivial scale-invariance limits. It has also been emphasized<sup>5,8</sup> that the correct sign for  $\Delta m$ , if it is finite, can come only from the subtraction term, because  $\Delta m(\text{Born})$  is known to be of the wrong sign, while the SLAC-MIT data on the structure functions indicate conclusively that the remaining inelastic contribution  $\Delta m^f$  is also of the wrong sign. Thus, in the Cottingham approach, the subtraction term in  $t_1(-Q^2, \nu)$  plays a crucial role in canceling<sup>7,9</sup> the logarithmic divergence in the self-mass  $\delta m$  to make it finite as well as leading to a correct sign for the mass difference  $\Delta m$ .

In this paper we propose a model of the forward (virtual) Compton amplitude which is taken to be the sum of the contributions from the poles and the cuts and exhibits all the usual analytic and invariant properties. The cut contribution is obtained in a novel way by mapping the cuts to a circle and

subjecting them to Regge constraints. The subtraction term is evaluated in terms of measurable quantities from an ansatz which is consistent with experiments and theoretical considerations. A few parameters are obtained by matching the electro-production data. The  $p$ - $n$  mass difference calculated by our parametrization scheme agrees quite well with experiments. The paper is organized as follows: In Sec. II we describe the kinematics and state the formula for the self-mass in terms of the forward (virtual) Compton amplitude. The various properties of the invariant Compton amplitudes  $t_i(\nu, Q^2)$  are listed and the relation of the latter to the inelastic structure functions is shown. In this section we also note the general condition for convergence of the Cottingham integral for the mass difference in presence of Bjorken scaling. Expressions for the invariant amplitudes are presented in Sec. III, using a variable obtained by the method of conformal mapping. Section IV deals with the various results of our model and describes the fits to the experimental data. In Sec. V we propose an ansatz and evaluate the subtraction term  $t_1(-Q^2, 0)$  in terms of measurable quantities. The final calculation of the  $p$ - $n$  mass difference using the Cottingham formula is made in this section. A brief summary of the results and some discussions are made in the concluding section, VI.

## II. PROPERTIES OF THE INVARIANT AMPLITUDES AND FORMULA FOR THE MASS DIFFERENCE

To lowest order in the electromagnetic interaction and to all orders in the strong interaction, the electromagnetic self-mass of a hadron can be ex-

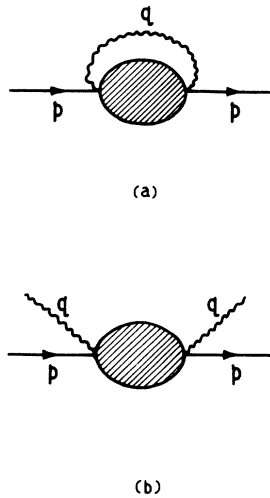


FIG. 1. (a) The lowest-order contribution to the electro-magnetic self-energy of a hadron. (b) The associated forward (virtual) Compton amplitude.

pressed as an integral over the forward Compton amplitude for scattering of the virtual photon off the hadron (Fig. 1):

$$\delta m = \frac{i}{(2\pi)^2} \int_{-\infty}^{+\infty} \frac{d^4 q}{q^2 + i\epsilon} g^{\mu\nu} T_{\mu\nu}(\vec{q}, \nu), \quad (1)$$

where  $\epsilon^\mu T_{\mu\nu} \epsilon^\nu$  is the forward Compton amplitude for scattering of photons of four-momentum  $q$  and polarization  $\epsilon$  off a hadron of four-momentum  $p$ ,  $m$  is the mass of the hadron, and  $\nu = p \cdot q/m$  is the photon energy in the laboratory frame.  $T_{\mu\nu}(\vec{q}, \nu)$  can be expanded in terms of two Lorentz-invariant functions of  $q^2$  and  $\nu$  as

$$T_{\mu\nu}(\vec{q}, \nu) = (q^2 g_{\mu\nu} - q_\mu q_\nu) t_1(q^2, \nu) + \left( -\nu^2 g_{\mu\nu} + \frac{\nu}{m} (p_\mu q_\nu + p_\nu q_\mu) - \frac{q^2 p_\mu p_\nu}{m^2} \right) t_2(q^2, \nu) \quad (2)$$

or, alternatively, as

$$T_{\mu\nu}(\vec{q}, \nu) = (\alpha/\pi) \left[ \frac{1}{m^2} \left( p_\mu - \frac{p \cdot q}{q^2} q_\mu \right) \left( p_\nu - \frac{p \cdot q}{q^2} q_\nu \right) T_2(q^2, \nu) - \left( g_{\mu\nu} - \frac{q_\mu q_\nu}{q^2} \right) T_1(q^2, \nu) \right] \quad (3)$$

such that  $T_{\mu\nu}(q, \nu)$  is manifestly gauge invariant,

$$q^\mu T_{\mu\nu} = q^\nu T_{\mu\nu} = 0, \quad (4)$$

which also guarantees

$$T_{\mu\nu} = T_{\nu\mu}. \quad (5)$$

The two sets of invariant amplitudes  $t_i$  and  $T_i$  are related linearly:

$$T_1(q^2, \nu) = (\pi/\alpha) [\nu^2 t_2(q^2, \nu) - q^2 t_1(q^2, \nu)] \quad (6a)$$

and

$$T_2(q^2, \nu) = -(\pi/\alpha) q^2 t_2(q^2, \nu), \quad (6b)$$

where  $\alpha = e^2/(4\pi)$  is the fine-structure constant.

### (i) $\nu$ -plane analyticity<sup>4,11</sup>

The invariant amplitudes  $t_i(q^2, \nu)$  for the nucleon case have the nucleon poles located at  $\nu = \pm(\nu_p - i\epsilon)$ , where  $\nu_p$  is given by

$$(\nu + q)^2 = m^2 + q^2 + 2\nu_p m = m^2, \quad (7a)$$

$$\text{i.e., } \nu_p = -q^2/2m$$

and cuts starting from the one-nucleon-one-meson branch points at  $\nu = \pm(\nu_c - i\epsilon)$ , where  $\nu_c$  is given by

$$(\nu + q)^2 = m^2 + q^2 + 2\nu_c m = (m + m_\pi)^2, \quad (7b)$$

$$\text{i.e., } \nu_c = \frac{-q^2 + m^2 + 2m m_\pi}{2m},$$

where  $m_\pi$  is the mass of the  $\pi$  meson.

The amplitudes  $t_i(q^2, \nu)$  are thus real analytic functions in the cut  $\nu$  plane with two poles (Fig. 2).

(ii) *s-u crossing*

In terms of the Mandelstam variables  $s = (p+q)^2 = m^2 + 2m\nu + q^2$  and  $u = (p-q)^2 = m^2 - 2m\nu + q^2$ , interchanging  $s \rightarrow u$  means changing the sign of  $\nu$ , so that

$$t_i(q^2, -\nu) = t_i(q^2, \nu) \quad (8)$$

implies  $s-u$  symmetry.<sup>4</sup> The  $t_i$ 's are therefore even functions of  $\nu$ .

(iii) *Regge behavior*

In the Regge limit ( $\nu \rightarrow \infty$ ,  $q^2$  fixed)  $t_1$  and  $\nu^2 t_2$  have the same asymptotic behavior,<sup>5</sup> which is given

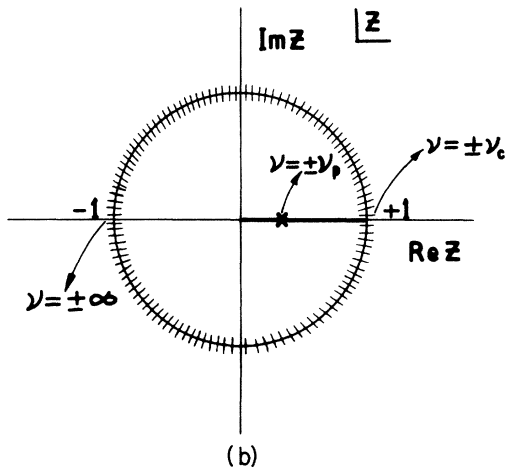
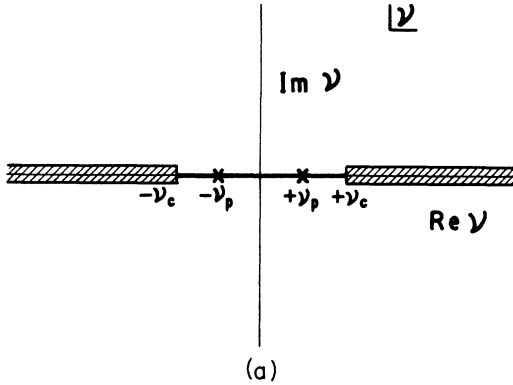


FIG. 2. (a) The conformal mapping of the cut  $\nu$  plane of analyticity of amplitudes  $t_i$  at fixed  $Q^2$  into the interior of (b) a unit circle in the  $Z$  plane.  $\nu_c$  and  $\nu_p$  are defined in the text, and corresponding regions in the  $\nu$  and  $Z$  planes have been shown.

by<sup>12</sup>

$$t_1(q^2, \nu) \xrightarrow[\nu \rightarrow \infty]{q^2 \text{ fixed}} \sum_j \gamma_j(q^2) \nu^{\alpha_j \xi_j}$$

and

$$\nu^2 t_2(q^2, \nu) \xrightarrow[\nu \rightarrow \infty]{q^2 \text{ fixed}} \sum_j \beta_j(q^2) \nu^{\alpha_j \xi_j},$$

where

$$\xi_j = (1 + e^{-i\pi\alpha_j}) / \sin(\pi\alpha_j) \quad (10)$$

are the signature factors and  $\alpha_j$  are the ( $t=0$ ) intercepts of the relevant Regge trajectories in the  $t$  channel [namely the  $P$ ,  $P'$ ,  $A_2$ , and  $A_2'$  trajectories<sup>15,16</sup> in the nucleon case which have  $I=0,1$  parity (+) and  $c=+1$ ].  $I$ -spin conservation at the  $NN$  Regge-pole vertex leads to the following relations<sup>4</sup> between the proton and neutron residue functions  $\beta_j^{p,n}(q^2)$  and  $\gamma_j^{p,n}(q^2)$ :

$$\begin{aligned} (\beta, \gamma)_P^p &= (\beta, \gamma)_P^n, \\ (\beta, \gamma)_{P'}^p &= (\beta, \gamma)_{P'}^n, \end{aligned} \quad (11)$$

and

$$(\beta, \gamma)_{A_2, A_2'}^p = -(\beta, \gamma)_{A_2, A_2'}^n.$$

(iv) *Fixed- $q^2$  dispersion relations*

The analyticity properties in  $\nu$  for fixed  $q^2$  and the asymptotic behavior in the Regge limit enable one to write down the fixed- $q^2$ , unsubtracted dispersion relation for  $t_2(q^2, \nu)$  and the once-subtracted dispersion relation for  $t_1(q^2, \nu)$  (see Ref. 5):

$$t_2(q^2, \nu) = \frac{2}{\pi} \int_0^\infty \frac{\nu' d\nu' \text{Im} t_2(q^2, \nu')}{\nu'^2 - \nu^2} \quad (12a)$$

and

$$t_1(q^2, \nu) = t_1(q^2, 0) + \frac{2\nu^2}{\pi} \int_0^\infty \frac{d\nu' \text{Im} t_1(q^2, \nu')}{\nu'(\nu'^2 - \nu^2)}. \quad (12b)$$

The Born contribution of the nucleon poles at  $\nu = \pm\nu_p$  can be separated by noting that

$$\text{Im} t_i(q^2, \nu') \Big|_{\nu' = \pm\nu_p} = 2\nu_p \pi \times \delta(\nu'^2 - \nu_p^2) f_i(q^2),$$

where  $f_i(q^2)$  are the residues at the poles, to obtain

$$t_2(q^2, \nu) = \frac{4mq^2 f_2(q^2)}{4m^2 \nu^2 - q^4} + \frac{2}{\pi} \int_{\nu_c}^\infty \nu' d\nu' \frac{\text{Im} t_2(q^2, \nu')}{\nu'^2 - \nu^2} \quad (13a)$$

$$\equiv t_{2B}(q^2, \nu) + t_2^I(q^2, \nu) \quad (13b)$$

and

$$\begin{aligned} t_1(q^2, \nu) &= t_1(q^2, 0) + \frac{16m^3 \nu^2 f_1(q^2)}{q^2(4m^2 \nu^2 - q^4)} \\ &+ \frac{2\nu^2}{\pi} \int_{\nu_c}^\infty d\nu' \frac{\text{Im} t_1(q^2, \nu')}{\nu'(\nu'^2 - \nu^2)} \end{aligned} \quad (14a)$$

$$\equiv t_1(q^2, 0) + t_{1B}(q^2, \nu) + t_1^I(q^2, \nu). \quad (14b)$$

The residues  $f_i(q^2)$  are related<sup>5,10</sup> to the nucleon electromagnetic form factors:

$$f_1^N(q^2) = \frac{(\alpha/\pi)[G_{MN}^2(q^2) - G_{EN}^2(q^2)]}{4m^2 - q^2} \quad (15)$$

and

$$f_2^N(q^2) = \frac{(\alpha/\pi)[q^2 G_{MN}^2(q^2) - 4m^2 G_{EN}^2(q^2)]}{q^2(4m^2 - q^2)} \quad (16)$$

where  $N$  stand for either  $p$  or  $n$  and  $G_M$  and  $G_E$  are the usual Sachs form factors for the nucleon.

(v) Relationship with the deep-inelastic structure functions

The deep-inelastic structure functions  $W_1(\nu, q^2)$  and  $W_2(\nu, q^2)$  are related by unitarity to the imaginary part of the forward Compton amplitudes for virtual photons,

$$W_i(\nu, -Q^2) = \pi^{-1} \text{Im} T_i(\nu, -Q^2), \quad (17)$$

and are measurable in  $eN$  (deep-inelastic) scattering for  $\nu > 0$  and  $q^2 \equiv -Q^2 < 0$ . The relation with  $t_i$  is obtained from (6a), (6b), and (17):

$$W_1(\nu, -Q^2) = (1/\alpha)[\nu^2 \text{Im} t_2(\nu, -Q^2) + Q^2 \text{Im} t_1(\nu, -Q^2)], \quad (18)$$

$$W_2(\nu, -Q^2) = (1/\alpha)Q^2 \text{Im} t_2(\nu, -Q^2). \quad (19)$$

The absorption cross section  $\sigma_T, \sigma_S$  for virtual photons with transverse and longitudinal polarizations, respectively, are related to the structure functions  $W_1$  and  $W_2$ :

$$W_1(\nu, -Q^2) = \left(\frac{K}{4\pi^2 \alpha}\right) \sigma_T, \quad (20a)$$

$$W_2(\nu, -Q^2) = \left(\frac{K}{4\pi^2 \alpha}\right) \left(\frac{Q^2}{Q^2 + \nu^2}\right) (\sigma_T + \sigma_S), \quad (20b)$$

where  $K = (W^2 - m^2)/2m$  and  $W^2 = 2m\nu - Q^2 + m^2$  is the invariant mass squared, such that

$$\frac{W_2}{W_1} = \left(\frac{Q^2}{Q^2 + \nu^2}\right) (1 + R), \quad (21)$$

where

$$R = R(\nu, -Q^2) = \sigma_S/\sigma_T. \quad (22)$$

From Eqs. (21), (18), and (19),  $R$  can be expressed in terms of  $\text{Im} t_i$ :

$$R(-Q^2, \nu) = \left(\frac{Q^2}{\nu^2}\right) \left(1 - \frac{\text{Im} t_1}{\text{Im} t_2}\right) / \left[1 + \frac{Q^2 \text{Im} t_1}{\nu^2 \text{Im} t_2}\right]. \quad (23)$$

Gauge invariance requires that in the real-photon limit ( $Q^2 \rightarrow 0$ ) the longitudinal cross section  $\sigma_S$  vanishes and  $\sigma_T \rightarrow \sigma_T(\gamma N)$ , where  $\sigma_T(\gamma N)$  is the total absorption cross section of real photons on the

nucleon. It follows that

$$R(-Q^2, \nu) \xrightarrow{Q^2 \rightarrow 0} 0 \quad (24)$$

and

$$\sigma_T(\gamma N) = \lim_{Q^2 \rightarrow 0} \left(\frac{4\pi^2 \alpha}{Q^2}\right) \nu W_2(\nu, -Q^2). \quad (25)$$

Equation (24) further implies that

$$\lim_{Q^2 \rightarrow 0} Q^2 \text{Im} t_1 = 0. \quad (26)$$

In general it has been shown<sup>5</sup> that not only the imaginary part of  $Q^2 t_1$  but also the real part vanishes,

$$\lim_{Q^2 \rightarrow 0} Q^2 \text{Re} t_1 = 0. \quad (27)$$

(vi) Scale invariance

Bjorken<sup>6</sup> had predicted that if one regards  $W_1$  and  $W_2$  as functions of variables  $Q^2$  and  $\omega = 2m\nu/Q^2$  then  $2mW_1$  and  $\nu W_2$  have the following nontrivial limits as  $Q^2 \rightarrow \infty$  with  $\omega$  fixed:

$$\lim_{\substack{Q^2 \rightarrow \infty \\ \omega \text{ fixed}}} \nu W_2(\nu, -Q^2) = F_2(\omega), \quad (28)$$

$$\lim_{\substack{Q^2 \rightarrow \infty \\ \omega \text{ fixed}}} 2mW_1(\nu, -Q^2) = F_1(\omega). \quad (29)$$

This remarkable property of the structure functions is known as scaling in the variable  $\omega$ , and the above limit ( $Q^2 \rightarrow \infty$ ,  $\omega$  fixed) is known as the Bjorken limit. As we shall see, scaling holds over a substantial portion of the ranges of  $\nu$  and  $Q^2$  investigated, in both proton and neutron cases. The structure functions and cross sections for the neutron are significantly less than those for the proton, indicating perhaps the presence of a nondiffractive contribution. Bjorken scaling as expressed by (28) and (29) severely constrains the behavior of  $\text{Im} t_i$  in the Bjorken limit:

$$\lim_{\substack{Q^2 \rightarrow \infty \\ \omega \text{ fixed}}} (1/\alpha) \nu Q^2 \text{Im} t_2(-Q^2, \nu) \equiv \lim_{\substack{Q^2 \rightarrow \infty \\ \omega \text{ fixed}}} \nu W_2(-Q^2, \nu) = F_2(\omega) \quad (30)$$

and

$$\lim_{\substack{Q^2 \rightarrow \infty \\ \omega \text{ fixed}}} (1/\alpha) [2m\nu^2 \text{Im} t_2(-Q^2, \nu) + 2mQ^2 \text{Im} t_1(-Q^2, \nu)] \equiv \lim_{\substack{Q^2 \rightarrow \infty \\ \omega \text{ fixed}}} 2mW_1(-Q^2, \nu) = F_1(\omega). \quad (31)$$

The following observations are crucial. From (31) and (30) we note that in general<sup>17</sup>

$$2mW_1 = \omega(\nu W_2) + G \quad (32a)$$

and hence

$$F_1(\omega) = \omega F_2(\omega) + \lim_{\substack{Q^2 \rightarrow \infty \\ \omega \text{ fixed}}} G(\nu, -Q^2), \quad (32b)$$

where

$$G(\nu, -Q^2) = (1/\alpha)2mQ^2 \text{Im}t_1(\nu, -Q^2). \quad (33)$$

The function  $G$  will help in calculating the subtraction constant from a simple ansatz, as is discussed

later.

We conclude this section by writing the "Wick-rotated Cottingham formula" for the mass difference  $\Delta m = \delta m_p - \delta m_n$  obtained<sup>4,10</sup> from (1) by the rotation<sup>19</sup>  $q^0 \rightarrow iq^0$ , i.e.,  $\nu \rightarrow i\nu$  (in the lab frame):

$$\Delta m = -\frac{1}{2\pi} \int_0^\infty \frac{dQ^2}{Q^2} \int_0^{(Q^2)^{1/2}} d\nu (Q^2 - \nu^2)^{1/2} [3Q^2 \Delta t_1(-Q^2, i\nu) - (Q^2 + 2\nu^2) \Delta t_2(-Q^2, i\nu)], \quad (34)$$

where  $\Delta t_i = t_i^p - t_i^n$  ( $i=1, 2$ ). This is the Cottingham formula.<sup>4</sup>

The  $t_i(-Q^2, i\nu)$  can then be represented by integrals over their imaginary parts by means of the fixed- $q^2$  dispersion relation (13) and (14), which are, for the present case of spacelike virtual photons, related [Eqs. (18) and (19)] to the experimentally accessible inelastic structure functions and nucleon form factors. One then obtains  $\Delta m$  in the form

$$\Delta m = \Delta m_B + \Delta m_I + \Delta m_{\text{sub}}, \quad (35)$$

where

$$\Delta m_B = -\frac{1}{2\pi} \int_0^\infty \frac{dQ^2}{Q^2} \int_0^{(Q^2)^{1/2}} d\nu (Q^2 - \nu^2)^{1/2} [3Q^2 \Delta t_{1B}(-Q^2, i\nu) - (Q^2 + 2\nu^2) \Delta t_{2B}(-Q^2, i\nu)] \quad (36)$$

is the contribution from the  $t_{iB}$ , defined by Eqs. (13b) and (14b) and  $\Delta m_I$  is given by<sup>8</sup>

$$\begin{aligned} \Delta m_I &= (\alpha/2\pi) \int_0^\infty \frac{dQ^2}{Q^2} \int_{\nu_c}^\infty \nu d\nu \left( 3\Delta W_1(-Q^2, \nu) \left[ 1 - \left( 1 + \frac{Q^2}{\nu^2} \right)^{1/2} + \frac{Q^2}{2\nu^2} \right] \right. \\ &\quad \left. + \Delta W_2(-Q^2, \nu) \left\{ \left( 1 + \frac{Q^2}{\nu^2} \right)^{1/2} - \frac{\nu^2}{Q^2} \left[ 1 - \left( 1 + \frac{Q^2}{\nu^2} \right)^{1/2} \right] - \frac{3}{2} \right\} \right) \\ &\equiv \int_0^\infty \frac{dQ^2}{Q^2} B(Q^2). \end{aligned} \quad (37)$$

Finally,  $\Delta m_{\text{sub}}$  is a contribution from the subtraction term given by<sup>10</sup>

$$\begin{aligned} \Delta m_{\text{sub}} &= -\frac{1}{2\pi} \int_0^\infty \frac{dQ^2}{Q^2} \int_0^{(Q^2)^{1/2}} d\nu (Q^2 - \nu^2)^{1/2} \\ &\quad \times [3Q^2 \Delta t_1(-Q^2, 0)] \\ &= -\frac{3}{8} \int_0^\infty dQ^2 Q^2 \Delta t_1(-Q^2, 0). \end{aligned} \quad (38)$$

Thus, to calculate  $\Delta m$ ,  $\Delta t_i(-Q^2, 0)$  is the only piece that remains to be evaluated in terms of experimentally determinable quantities. We take this up in Sec. V.

Before concluding this section we note the condition that the deep-inelastic contribution for the mass difference does not diverge because it is well known<sup>7-9</sup> that the latter quantity is, in general, logarithmically divergent in the presence of Bjorken scaling. The coefficient of the logarithmic divergence is given by<sup>9</sup>

$$\begin{aligned} \Delta &= \lim_{Q^2 \rightarrow \infty} -\frac{3}{8} Q^4 \Delta t_1'(-Q^2, 0) \\ &\quad + \frac{3\alpha m}{8\pi} \int_0^1 dx [\Delta F_2(x) + 2x \Delta F_1(x)], \end{aligned} \quad (39a)$$

where  $x=1/\omega$  and the superscript  $I$  signifies inelastic contribution. Therefore, the logarithmic divergence disappears only if<sup>9</sup>  $\Delta=0$ , i.e.,

$$\lim_{Q^2 \rightarrow \infty} \frac{3}{8} Q^4 \Delta t_1'(-Q^2, 0) = \frac{3\alpha m}{8\pi} \int_0^1 dx [\Delta F_2(x) + 2x \Delta F_1(x)]. \quad (39b)$$

We show in Sec. IV and V how this condition is realized. It is consistent with the theoretical considerations and the experimental data, thus rendering the mass difference finite, and is an achievement of our analytic model.

### III. MODEL FOR $t_1$ AND $t_2$

In this section we present our parametrization for  $t_1$  and  $t_2$ . Consider the conformal mapping

$$Z = \frac{1 - (1 - \nu^2/\nu_c^2)^{1/2}}{1 + (1 - \nu^2/\nu_c^2)^{1/2}} = \frac{1 - (1 - \omega^2/\omega_c^2)^{1/2}}{1 + (1 - \omega^2/\omega_c^2)^{1/2}}, \quad (40)$$

where

$$\omega_c \equiv \frac{\nu_c}{\nu_p} = \frac{Q^2 + 2mm_\pi + m_\pi^2}{Q^2} \quad \text{and} \quad \omega \equiv \frac{\nu}{\nu_p} = \frac{2m\nu}{Q^2}. \quad (41)$$

$\omega$  is the scaling variable.  $Z$  is real for  $\nu^2 \leq \nu_c^2$  and has square-root branch points at  $\nu = \pm \nu_c$  at

which it is unity. For  $\nu^2 > \nu_c^2$ ,  $Z$  can be expressed as

$$Z = \frac{1+iX}{1-iX}$$

with

$$X = \left( \frac{\omega^2}{\omega_c^2} - 1 \right)^{1/2}, \quad Z_R = \frac{1-X^2}{1+X^2}; \quad Z_I = \frac{2X}{1+X^2} \quad (42)$$

such that  $ZZ^* = Z^*Z = 1$ .

In this way the cut- $\nu$  plane is mapped into the interior of a unit circle in the  $Z$  plane with center at the origin (Fig. 2). The analytic structure of the amplitudes  $t_i$  in  $\nu$  is thus guaranteed by expressing these as functions in  $Z$ . We define

$$Z_\rho = Z(\nu = \nu_\rho) = \frac{1 - (1 - \nu_\rho^2/\nu_c^2)^{1/2}}{1 + (1 - \nu_\rho^2/\nu_c^2)^{1/2}}, \quad (43)$$

which has the interesting property that  $Z_\rho = 0$  at  $Q^2 = 0$  and  $Z_\rho \rightarrow 1$  as  $Q^2 \rightarrow \infty$ . Before presenting our model we list some other useful properties and uses of this variable which are suitable for the present problem.

(i)  $Z$  is dimensionless and  $Z \equiv Z(\omega, \omega_c) \equiv Z(\omega/\omega_c)$ . Since  $\omega_c \rightarrow Q^2 \rightarrow \infty$ ,  $Z(\omega/\omega_c) \rightarrow Z(\omega)$ , showing it to be a natural choice as a variable to incorporate

Bjorken scaling into the theory. At finite  $Q^2$ ,  $\omega_c$  could be a measure of the scale-invariance breaking.

(ii) The Drell-Yan-West<sup>20</sup>-type threshold behavior of the structure functions is readily generated by the combination  $|(Z_\rho - Z)/(Z_\rho + 1)|^{2l}$  which behaves near the threshold as  $(\omega^2 - 1)^l$  in the scale-invariance limit ( $Q^2 \rightarrow \infty$ ,  $\omega$  fixed) and at the same time tends to unity at large  $\omega$ , thus leaving the high-energy behavior unaffected.

(iii) One can incorporate the asymptotic Regge behavior [Eqs. (9), (10)] by noting that

$$(1+Z)^{-\alpha} = \left( \frac{\nu}{2\nu_c} \right)^\alpha e^{-i\alpha \tan^{-1}(\nu^2/\nu_c^2 - 1)^{1/2}} \xrightarrow[Q^2 \text{ fixed}]{\nu \rightarrow \infty} \left( \frac{\nu}{2\nu_c} \right)^\alpha e^{i\alpha\pi/2}.$$

(iv)  $Z$  is an even function in  $\nu$  (or  $\omega$ ), i.e.,  $Z(-\nu) = Z(\nu)$ , such that the  $s$ - $u$  crossing symmetry [Eq. (8)] can be taken into account.

(v)  $Z(i\nu)$  is real.

The properties indicated above lead us to express  $t_{1,2}^{\rho,n}$  as follows (assume these to contain all information about the  $\text{Im } t_{1,2}^{\rho,n}$ ):

$$t_2^{\rho,n}(-Q^2, \nu) \simeq \frac{4m}{Q^4 - 4m^2\nu^2} \left[ Q^2 f_2^{\rho,n}(-Q^2) + \left| \frac{Z_\rho - Z}{Z_\rho + 1} \right|^{2l_{\rho,n}} \sum_j \beta_j^{\rho,n} \frac{(1+Z)^{-\alpha_j}}{\sin(\alpha_j\pi/2)} \right] \quad (44)$$

$$t_1^{\rho,n}(-Q^2, \nu) \simeq t_1^{\rho,n}(-Q^2, 0) + \frac{4m(\nu^2/\nu_c^2)}{Q^4 - 4m^2\nu^2} \left[ \frac{4m^2\nu_c^2}{Q^2} f_1^{\rho,n}(-Q^2) + \left| \frac{Z_\rho - Z}{Z_\rho + 1} \right|^{2l_{\rho,n}} g(Q^2, \nu) \sum_j \gamma_j^{\rho,n} \frac{(1+Z)^{-\alpha_j}}{\sin(\alpha_j\pi/2)} \right], \quad (45)$$

where

$$g(Q^2, \nu) = \exp[-(Q_0^2/Q^2)^k |1+Z|]. \quad (46)$$

$l_\rho$ ,  $l_n$ , and  $k$  are integers,<sup>21</sup> and  $\alpha_j = \alpha_j(t=0)$  are the ( $t=0$ ) intercepts of the relevant Regge trajectories, i.e.,  $j=P, P', A_2$ , and  $A_2'$ . We assume<sup>15,16</sup>  $\alpha_P = 1.0$ ,  $\alpha_{P'} = \alpha_{A_2} = \frac{1}{2}$ , and  $\alpha_{A_2'} = \alpha_{A_2} - 1.0$ . The  $(\beta, \gamma)_j^{\rho,n}$  which are chosen independent of  $Q^2$  are subject to the constraints<sup>14</sup> given by (11), which reduce their number from sixteen to only eight, viz.,  $\beta_P (\equiv \beta_P^{\rho,n} = \beta_P^n)$ ,  $\beta_{P'} (\equiv \beta_{P'}^{\rho,n} = \beta_{P'}^n)$ ,  $\beta_{A_2} (\equiv \beta_{A_2}^{\rho,n} = -\beta_{A_2}^n)$ , and  $\beta_{A_2'} (\equiv \beta_{A_2'}^{\rho,n} = -\beta_{A_2'}^n)$ , and similarly for the  $\gamma$ 's.

The exponential factor  $g(Q^2, \nu)$  has been included in the parametrization for  $t_1$  in order to reproduce the significant departure from scale invariance at  $\omega > 5$ , as exhibited by the recent data<sup>34</sup> on  $\nu R_\rho$  (Sec. IV). It is to be noticed that the factor  $g(Q^2, \nu)$  has been so chosen that the scaling limit ( $Q^2 \rightarrow \infty$ ) and the Regge limit ( $\nu \rightarrow \infty$ ) are both left undisturbed while the departure from scaling at finite  $Q^2$  is characterized by the parameter  $Q_0^2$ . The  $t_2^N$  are built up in our representation as the sum of the contribution from the nucleon poles (i.e., the Born term) and the inelastic contribution, while the  $t_1^N$  contain extra pieces which are the subtraction terms. Thus, we have

$$t_2^N = t_{2B}^N + t_{2I}^N$$

and

$$t_1^N = t_{1 \text{ sub}}^N + t_{1B}^N + t_{1I}^N.$$

The structure functions  $\nu W_2^N$  and  $2mW_1^N$ , which are conjectured to exhibit scaling, are obtained from imaginary parts of the  $t_i^N$  according to (18) and (19):

$$\begin{aligned} \nu W_2^{\rho,n}(-Q^2, \omega) &= \frac{1}{\alpha} \left( \frac{2\omega}{1-\omega^2} \right) \left| \frac{Z_\rho - Z}{Z_\rho + 1} \right|^{2l_{\rho,n}} \text{Im} \left[ \sum_j \beta_j^{\rho,n} \frac{(1+Z)^{-\alpha_j}}{\sin(\alpha_j \pi/2)} \right] \\ &= \frac{1}{\omega \geq \omega_c} \frac{1}{\alpha} \left( \frac{2\omega}{1-\omega^2} \right) \left| \frac{Z_\rho - Z}{Z_\rho + 1} \right|^{2l_{\rho,n}} \sum_j \beta_j^{\rho,n} \left( \frac{\omega}{2\omega_c} \right)^{\alpha_j} \frac{\sin(-\alpha_j \theta)}{\sin(\alpha_j \pi/2)} \end{aligned} \quad (47)$$

and

$$2mW_1^{\rho,n} = \omega(\nu W_2^{\rho,n}) + G^{\rho,n} \quad (48)$$

with

$$\begin{aligned} G^{\rho,n}(-Q^2, \omega) &\equiv (1/\alpha) 2mQ^2 \text{Im} t_1(-Q^2, \omega) \\ &= \left( \frac{1}{\alpha} \right) \frac{8m^2 \omega^2 / \omega_c^2}{Q^2(1-\omega^2)} \left| \frac{Z_\rho - Z}{Z_\rho + 1} \right|^{2l_{\rho,n}} g(Q^2, \omega) \sum_j \gamma_j^{\rho,n} \left( \frac{\omega}{2\omega_c} \right)^{\alpha_j} \frac{\sin(-\alpha_j \theta)}{\sin(\alpha_j \pi/2)}, \end{aligned} \quad (49)$$

where

$$\theta = \theta(-Q^2, \omega) = \tan^{-1}(\omega^2 / \omega_c^2 - 1)^{1/2}. \quad (50)$$

It is worthwhile to examine whether the expressions (44)–(45) satisfy the various properties of the  $t_1^N$  listed in Sec. II.

By virtue of the conformal mapping  $Z$ , the analytic structure in the  $\nu$  plane [Sec. II(i)], is explicitly built into the amplitudes  $t_i^N$ . In the limit  $\nu \rightarrow \pm(\nu_\rho)$ , i.e.,  $Z \rightarrow Z_\rho$ , one recovers the Born amplitudes  $t_{iB}$  with appropriate residues  $f_i(Q^2)$  at the poles. The  $s$ - $u$  crossing symmetry is automatically incorporated by the variable  $Z$ . To examine asymptotic behavior in the Regge limit, we note that using the property of  $Z$  as given by Sec. III(iii) we have

$$\lim_{\substack{\nu \rightarrow \infty \\ Q^2 \text{ fixed}}} \nu^2 t_2^N(-Q^2, \nu) = \sum_j \beta_j^N(-Q^2) \nu^{\alpha_j} \xi_j,$$

$$\lim_{\substack{\nu \rightarrow \infty \\ Q^2 \text{ fixed}}} t_1^N(-Q^2, \nu) = \sum_j \gamma_j^N(-Q^2) \nu^{\alpha_j} \xi_j,$$

where the Regge residue functions  $\beta_j^N(-Q^2)$  and  $\gamma_j^N(-Q^2)$  are given by  $\beta_j^N(-Q^2) = (2\nu_c)^{-\alpha_j} \beta_j^N$  and similarly for  $\gamma_j^N(-Q^2)$ , and

$$\begin{aligned} \xi_j &= \frac{e^{-i\alpha_j \pi/2}}{\sin(\frac{1}{2}\pi \alpha_j)} \\ &= \left( \frac{1 + e^{-i\alpha_j \pi}}{\sin(\alpha_j \pi)} \right) \end{aligned}$$

is the signature factor. The factorization of the Regge residue functions in the above manner signifies that the Regge behavior at finite  $Q^2$  is extended<sup>15,16</sup> into the scaling region ( $Q^2 \rightarrow \infty$ ,  $\nu \rightarrow \infty$  with  $\omega$  fixed) (Eqs. 47–49).  $I$ -spin conservation at the  $NN$  Regge-pole vertex is satisfied by our choice of  $\beta_j^N, \gamma_j^N$  subject to the constraints (11).

In the Bjorken-scaling limit ( $Q^2 \rightarrow \infty$ ,  $\omega$  fixed  $\geq 1$ ) the electroproduction structure functions  $\nu W_2(\omega, -Q^2)$  and  $2mW_1(\omega, -Q^2)$  become scale invari-

ant and are given by

$$\begin{aligned} \lim_{\substack{Q^2 \rightarrow \infty \\ \omega \text{ fixed} \geq 1}} \nu W_2^{\rho,n}(-Q^2, \omega) &= F_2^{\rho,n}(\omega) \\ &= \frac{1}{\alpha} \left( \frac{2\omega}{1-\omega^2} \right) \left( \frac{\omega^2 - 1}{\omega^2} \right)^{l_{\rho,n}} \\ &\quad \times \sum_j \beta_j^{\rho,n} \frac{\omega^{\alpha_j} \sin[-\alpha_j \tan^{-1}(\omega^2 - 1)^{1/2}]}{2^{\alpha_j} \sin(\alpha_j \pi/2)}, \end{aligned} \quad (51)$$

$$\begin{aligned} \lim_{\substack{Q^2 \rightarrow \infty \\ \omega \text{ fixed} \geq 1}} 2mW_1^{\rho,n}(-Q^2, \omega) &= F_1^{\rho,n}(\omega) \\ &= \omega F_2^{\rho,n}(\omega). \end{aligned} \quad (52)$$

The functions  $F_2^{\rho,n}(\omega)$  and  $F_1^{\rho,n}(\omega)$ , as defined above, have the following *threshold behavior* ( $\lim \omega \rightarrow 1$ ):

$$F_{1,2}^{\rho,n}(\omega) \underset{\omega \rightarrow 1}{\sim} (\omega - 1)^{l_{\rho,n} - 1/2}, \quad (53)$$

which is very similar to the Drell-Yan-West<sup>20</sup>-type behavior. This aspect is further discussed in Sec. V, where we describe the fits to the electroproduction data. It may also be noted that in the real-photon limit ( $Q^2 \rightarrow 0$ ),  $Q^2 t_1$  and  $R$  vanish, while according to (25)

$$\lim_{Q^2 \rightarrow 0} (4\pi^2 \alpha / Q^2) \nu W_2^N(\nu, -Q^2) = \sigma_T(\gamma N)$$

are the total absorption cross sections of real photons on the nucleon  $N$ . The prediction of our model for these cross sections agrees quite well (Sec. V and Fig. 10) with the available data.

#### IV. FITS TO THE EXPERIMENTAL DATA AND EVALUATION OF THE PARAMETERS OF THE MODEL

Using the representations for  $\nu W_2^{\rho,n}$ ,  $2mW_1^{\rho,n}$ ,  $R_\rho$ , and  $\Delta t_i(-Q^2, 0)$  [Eqs. (47)–(49), (23), and (62), re-

spectively] we have searched for a least-squares fit to the experimental data on  $\nu W_2^p$ ,  $2mW_1^p$ ,  $\nu W_2^p - \nu W_2^n$ ,  $\nu W_2^n/\nu W_2^p$ , and  $\nu R_p$  plotted as functions of  $\omega$  (or  $x=1/\omega$ , as the case is) for various fixed  $Q^2$  values, by varying the twelve parameters (i.e., the eight Regge parameters  $\beta_P, \beta_{P'}, \beta_{A_2}, \beta_{A_2'}, \gamma_P, \gamma_{P'}, \gamma_{A_2}, \gamma_{A_2}'$ , the two threshold exponents  $l_p, l_n$ , and the parameters  $k$  and  $Q_0^2$  occurring in  $t_1$ ) of our theory. The data selection and searching procedure is described below.

The structure functions  $W_2$  and  $W_1$  are separated from the cross-section measurements taken at two or more different angles (at the same values of  $Q^2$  and  $\nu$ ). Experimental data for  $\nu W_2^p$  and  $2mW_1^p$  as functions of  $(\omega, Q^2)$  exist over a kinematical range with  $W > 2.6$  (GeV/c),  $Q^2 > 1.0$  (GeV/c)<sup>2</sup>, and  $\omega < 12$ . This corresponds to a region in the  $W^2-Q^2$  plot (labeled Region I; cf. Ref. 23, Fig. 4) over which scaling in  $\omega$ ,<sup>24</sup> has been substantially verified. To each data point corresponds a value of  $\omega$  and a range of values of  $Q^2$ .<sup>23</sup> Since the complete set of data is not available to us in a tabulated form, we have chosen to select a subset of data points (55 points for  $\nu W_2^p$  and 42 points for  $2mW_1^p$ ) from the graphs<sup>23</sup> which are "representative" of the complete set (in the sense that a good fit to this subset is claimed to be a good fit to the complete set).

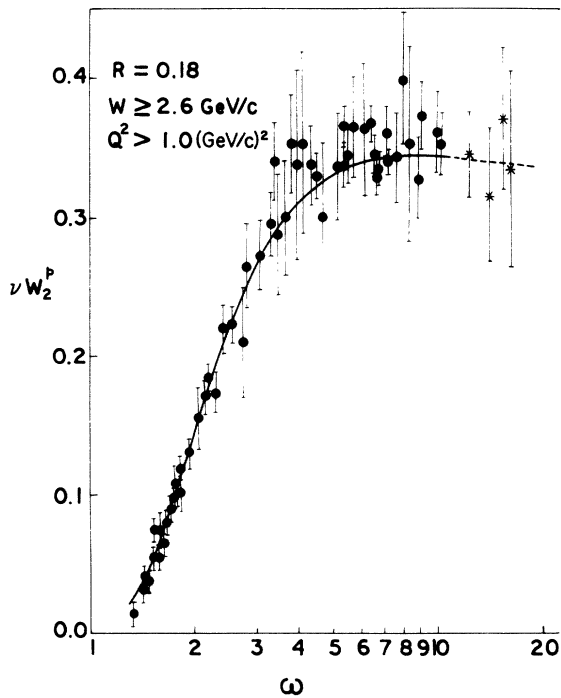


FIG. 3. Fit to the structure function  $\nu W_2^p(\omega, -Q^2)$ . The data are from Ref. 23. The starred points correspond to  $\omega > 12$  and the solid (dashed) curve represents our fit in the region  $\omega < (>) 12$ .

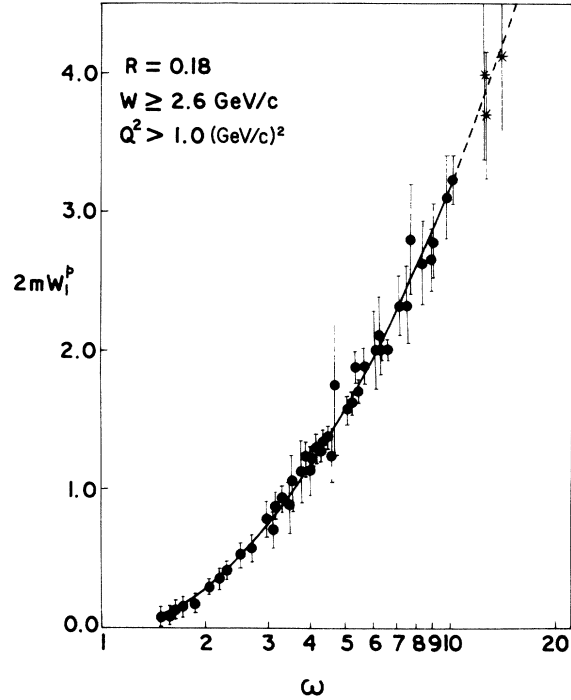


FIG. 4. Fit to the structure function  $2mW_1^p(\omega, -Q^2)$ . The data are from Ref. 23. The starred points correspond to  $\omega > 12$ , and the solid (dashed) curve denotes our fit in the region  $\omega < (>) 12$ .

The value of  $Q^2$  for each data point is chosen to be the maximum of the range (corresponding to the boundary of the region I, Fig. 4 of Ref. 23) in order that the Bjorken limiting procedure is followed as closely as possible. The 68 data points (34 each)

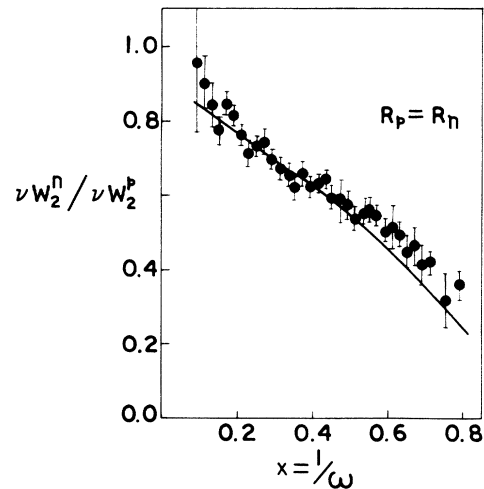


FIG. 5. Fit to the neutron-to-proton ratio  $\nu W_2^n/\nu W_2^p$  as a function of  $x (=1/\omega)$  for fixed values of  $Q^2$ . The data are from Ref. 22.



for  $\nu W_2^p - \nu W_2^n$  and  $\nu W_2^n / \nu W_2^p$  are from Ref. 22 and the 86 data points for  $\nu R_p$  from Ref. 34.

We then proceeded to make a random search for the parameters  $\beta_p, \beta_{p'}, \beta_{A_2}, \beta_{A_2'}, \gamma_p, \gamma_{p'}, \gamma_{A_2}, \gamma_{A_2}'$ , and  $Q_0^2, l_p, l_n$ , and  $k$  fixed at different integral values<sup>21</sup> that would minimize the total  $\chi^2$ .<sup>25</sup> The condition of convergence of the Cottingham-integral as given by Eq. (39) is used as a constraint in searching for the parameters.

The minimum value of  $\chi^2$  obtained was 317, for 252 data points with 12 parameters the values of which corresponding to this minimum  $\chi^2$  are as follow:

$$\begin{aligned}
 l_p &= 4, \\
 l_n &= 5, \\
 k &= 6, \\
 Q_0^2 &= 1.35 \text{ (GeV/c)}^2, \\
 \beta_p &= 2.15 \times 10^{-3}, \\
 \beta_{p'} &= 0.71 \times 10^{-3}, \\
 \beta_{A_2} &= 0.55 \times 10^{-3}, \\
 \beta_{A_2'} &= -0.09 \times 10^{-3}, \\
 \gamma_p &= -0.5626 \times 10^{-3}, \\
 \gamma_{p'} &= 0.7881 \times 10^{-3}, \\
 \gamma_{A_2} &= -0.3792 \times 10^{-3}, \\
 \gamma_{A_2'} &= 0.4107 \times 10^{-3}.
 \end{aligned} \tag{54}$$

Our fits are shown in Figs. 3-7. An examination of the parameters, thus determined, reveals the

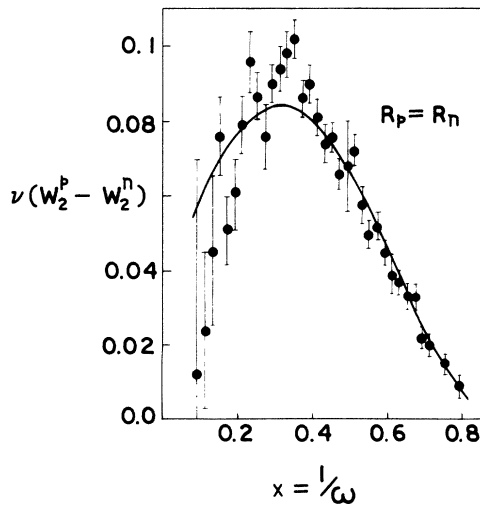


FIG. 6. Fit to the difference  $\nu W_2^p - \nu W_2^n$  as a function of  $x (=1/\omega)$  for fixed values of  $Q^2$ . The data are from Ref. 22.

following features of the model:

(a) The "proton" structure functions,  $\nu W_2^p$  and  $2mW_1^p$ , have a threshold behavior (Eq. 53)

$$\nu W_2^p, 2mW_1^p \underset{\omega \rightarrow 1}{\sim} (\omega - 1)^{3.5}, \tag{55}$$

and the "neutron" structure functions behave near threshold as

$$\nu W_2^n, 2mW_1^n \underset{\omega \rightarrow 1}{\sim} (\omega - 1)^{4.5}. \tag{56}$$

The existing data on the structure functions are thus consistent with threshold behavior other than<sup>26</sup>  $(\omega - 1)^3$ , which is prescribed by the Drell-Yan-West<sup>20</sup> relation if the nucleon electromagnetic form factor  $G_M(t)$  obeys a dipole behavior. Drell, Levy, and Yan<sup>27</sup> have shown that  $F_2(\omega) \sim (\omega - 1)^k$  near threshold with  $k$  even or odd if the electromagnetic current couples solely to spin-0 or spin- $\frac{1}{2}$  fields, respectively.

(b) In our model for  $\nu W_2^p$ , next-to-leading trajectories which give rise to a falloff like  $\omega^{-1/2}$  become unimportant for large  $\omega$  although they contribute significantly for small  $\omega$  ( $<5$ , say). The large- $\omega$  region is thus primarily diffractive in nature, and in the scale-invariance limit the Pom-eranchukon plateau corresponds to a value  $\approx 0.3$ , which is not much less than the maximum  $\approx 0.33$  attained in the model. We are thus led to agree with Harari's<sup>28</sup> suggestion that the high- $\omega$  region is mainly diffractive in nature and not with models<sup>29,30</sup> that predict significant nonleading contribution in this region. Further evidence for dominance of the diffractive component at large values of  $\omega$  is exhibited by the ratio and difference of proton and neutron structure functions, which we discuss below.

(c) An examination of the fits to  $\nu W_2^p - \nu W_2^n$  and  $\nu W_2^n / \nu W_2^p$  reveals that, for large  $\omega$ ,  $\nu W_2^n$  approaches  $\nu W_2^p$  quite rapidly and the two are equal within 10% at  $\omega \approx 10$ , but for small  $\omega$  there is a significant difference,  $(\nu W_2^p - \nu W_2^n) \sim \omega^{1/2}$ , showing dominant nondiffractive contribution. The value  $\nu W_2^n / \nu W_2^p$  is predicted to be 0.47 in a duality model<sup>30</sup> at  $\omega = 1$  and to be 0.25 as a lower bound in a quark model.<sup>31</sup> Our model appears to be consistent with the latter prediction.

(d) The fits to the recent data<sup>34</sup> on  $\nu R_p$  plotted as a function of  $Q^2$  to test the scale invariance of the latter are shown in Fig. 7. Clearly, there is significant departure from scale invariance at values of  $\omega > 5$  and  $Q^2 < 4 \text{ (GeV/c)}^2$ . Our fits give the value of  $\chi^2 = 112$  for the 86 data points.

With the parameters given above we obtain fits to (i) the data<sup>23</sup> of  $\nu W_2^p$  plotted as a function of  $Q^2$  for various fixed ranges of  $\omega$  (Fig. 8), which exhibit scale-invariance breaking at small  $Q^2$  (it is to be noted that unlike other Regge models<sup>14,15,16</sup> ours does not

need any additional mass parameter to characterize scale-invariance breaking of  $\nu W_2$  at finite  $Q^2$ , (ii) data<sup>23</sup> on  $1 + (\nu W_2^n / \nu W_2^p)$  plotted as a function of  $Q^2$  for various fixed values of  $W$  (Fig. 9), and (iii) the data<sup>32,33</sup> on total photoabsorption cross sections on protons and neutrons,  $\sigma_T(\gamma p)$ ,  $\sigma_T(\gamma n)$  as well as their differences:  $\sigma_T(\gamma p) - \sigma_T(\gamma n)$  as a function of the photon energy  $\nu$  (Fig. 10). The rapid approach of the photoabsorption cross section to their asymptotic value in our model is consistent with the Pommeranchukon dominance of  $\nu W_2$  at large  $\omega$  as discussed above. It should be emphasized that these fits are absolute predictions of our model.

#### V. EVALUATION OF THE SUBTRACTION TERM $\Delta t_1(-Q^2, 0)$ AND CALCULATION OF THE $p$ - $n$ MASS DIFFERENCE

We now turn to the problem of evaluating the subtraction piece in terms of the structure functions. With reference to the definition of  $R$  in terms of  $\text{Im} t_i^N$  [Eq. (23)], it can be shown that in the Regge limit ( $\nu \rightarrow \infty$ ,  $Q^2$  fixed) we have

$$\frac{R_\infty}{1 + R_\infty} = - \frac{Q^2 \text{Im} t_1}{\nu^2 \text{Im} t_2} \Big|_{Q^2 \text{ fixed}, \nu \rightarrow \infty}, \quad (57)$$

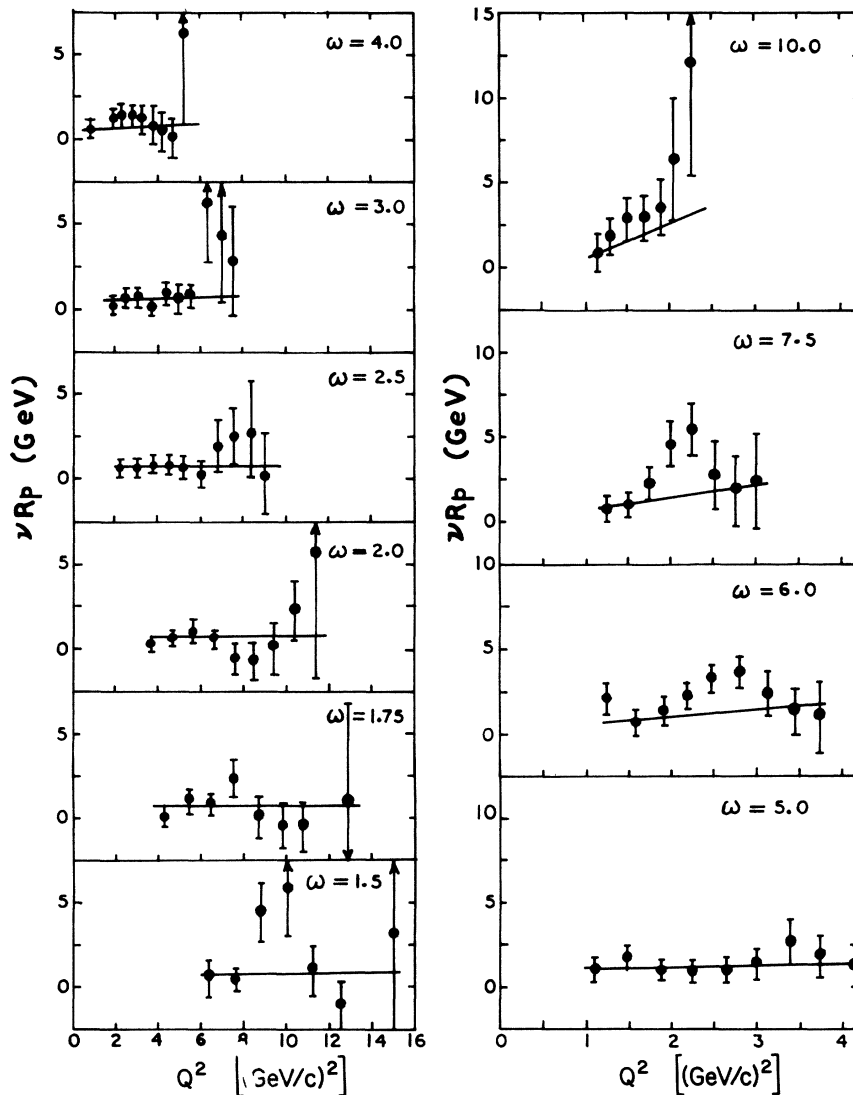


FIG. 7. The quantity  $\nu R_p$  versus  $Q^2$  for fixed values of  $\omega$ . The data are from Ref. 34. The solid curves are our fits.

where

$$R_\infty = R_\infty(Q^2) = \lim_{\substack{\nu \rightarrow \infty \\ Q^2 \text{ fixed}}} R(\nu, -Q^2)$$

is assumed to exist. Therefore, if we define

$$t_G(-Q^2, \nu) = t_1(-Q^2, \nu) + \frac{\nu^2}{Q^2} \left( \frac{R_\infty}{1+R_\infty} \right) t_2(-Q^2, \nu) \quad (58)$$

then

$$\text{Im}t_G(-Q^2, \nu) \xrightarrow[\nu \rightarrow \infty, Q^2 \text{ fixed.}]{\nu} 0 \quad (59)$$

by construction, and therefore  $t_G$  will satisfy an

unsubtracted fixed- $Q^2$  dispersion relation,

$$t_G(-Q^2, \nu) = \frac{2}{\pi} \int_0^\infty \frac{\text{Im}t_G(-Q^2, \nu') \nu' d\nu'}{\nu'^2 - \nu^2}, \quad (60)$$

but

$$t_1(-Q^2, 0) \equiv t_G(-Q^2, 0) = \frac{2}{\pi} \int_0^\infty \frac{\text{Im}t_G(-Q^2, \nu) d\nu}{\nu}. \quad (61)$$

The contribution from nucleon poles can be separated and the inelastic contribution can be represented as an integral over the structure functions  $W_1$  and  $W_2$ , and one obtains for  $\Delta t_1(-Q^2, 0)$

$$\begin{aligned} \Delta t_1(-Q^2, 0) &= \left( \frac{\alpha}{\pi} \right) \left\{ 4m\Delta f_1(-Q^2)/Q^2 + \Delta \left[ \frac{R_\infty}{1+R_\infty} f_2(-Q^2)/m \right] \right\} \\ &\quad + \left( \frac{\alpha}{\pi m Q^2} \right) \int_{\nu_c}^\infty \frac{d\nu}{\nu} \left\{ \Delta G(-Q^2, \nu) + \omega \Delta \left[ \left( \frac{R_\infty}{1+R_\infty} \right) \nu W_2 \right] \right\} \\ &\equiv \Delta t_1^{\text{poles}}(-Q^2, 0) + \Delta t_1^{\text{inelastic}}(-Q^2, 0), \end{aligned} \quad (62)$$

where  $f_i^N$  and  $G^N$  have been defined earlier in the text,  $\Delta t_1^{\text{poles}}(-Q^2, 0)$  is the contribution from the poles, and  $\Delta t_1^{\text{inelastic}}(-Q^2, 0)$  is the inelastic contribution. In our model,

$$\left( \frac{R_\infty}{1+R_\infty} \right)_N = - \left( \frac{Q^2}{\nu_c^2} \right) \frac{\sum_i \gamma_i^N (\nu/2\nu_c)^{\alpha_i}}{\sum_j \beta_j^N (\nu/2\nu_c)^{\alpha_j}}, \quad (63)$$

where  $N$  is  $p$  or  $n$  and the sum includes all the relevant ( $I=0$  and  $I=1$ ) trajectories,  $P$ ,  $P'$ ,  $A_2$ , and  $A_2'$ , such that Eq. (59) for  $\text{Im}t_G$ , i.e.,  $\text{Im}t_G \rightarrow 0$  for  $\nu \rightarrow \infty$ , holds rigorously to the order  $\nu^{-s}$  where  $s > \frac{1}{2}$ . Thus the subtraction constant  $\Delta t_1(-Q^2, 0)$  satisfies the limit<sup>5</sup>

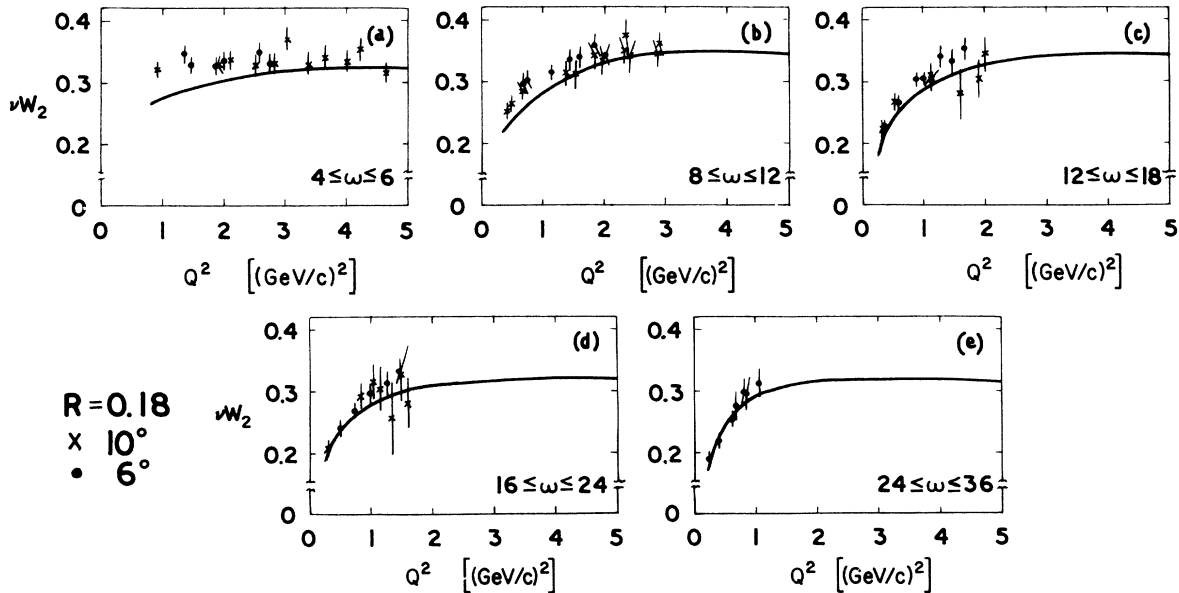


FIG. 8. Fit to  $\nu W_2^p$  as a function of  $Q^2$  for fixed values of  $\omega$ , showing scale-invariance breaking at small  $Q^2$ . Our fits (solid curves) are calculated by using the average value of  $\omega$  in the range indicated for each case. The data are from Bloom *et al.*, Ref. 23.

$$\begin{aligned} \lim_{Q^2 \rightarrow 0} Q^2 \Delta t_1(-Q^2, 0) &= \lim_{Q^2 \rightarrow 0} Q^2 \Delta t_1^{\text{poles}}(-Q^2, 0) \\ &= \frac{\alpha}{\pi m} (\mu_p^2 - \mu_n^2 - 1), \end{aligned} \quad (64)$$

where  $\mu_N$  are the magnetic moments of the nucleons. Further, the condition of convergence of the Cottingham integral as given by Eq. (39) is satisfied since the latter equation has been used as a constraint in obtaining the parameters given by (54). The validity of Eq. (39) is illustrated graphically in Fig. 11, which shows how the inelastic contribution of the subtraction term approaches

the desired limit in order to cancel the coefficient of possible logarithmic divergence.

Using our model for the structure functions  $W_i^{p,n}$  with parameters given by Eq. (54) and the dipole fit to the nucleon form factors,

$$G_{EP}(-Q^2) = \frac{G_{Mp}(-Q^2)}{\mu_p} = \frac{G_{Mn}(-Q^2)}{\mu_n} = \frac{1}{(1 + Q^2/0.71)^2} \quad (65)$$

and

$$G_{EN}(-Q^2) = 0,$$

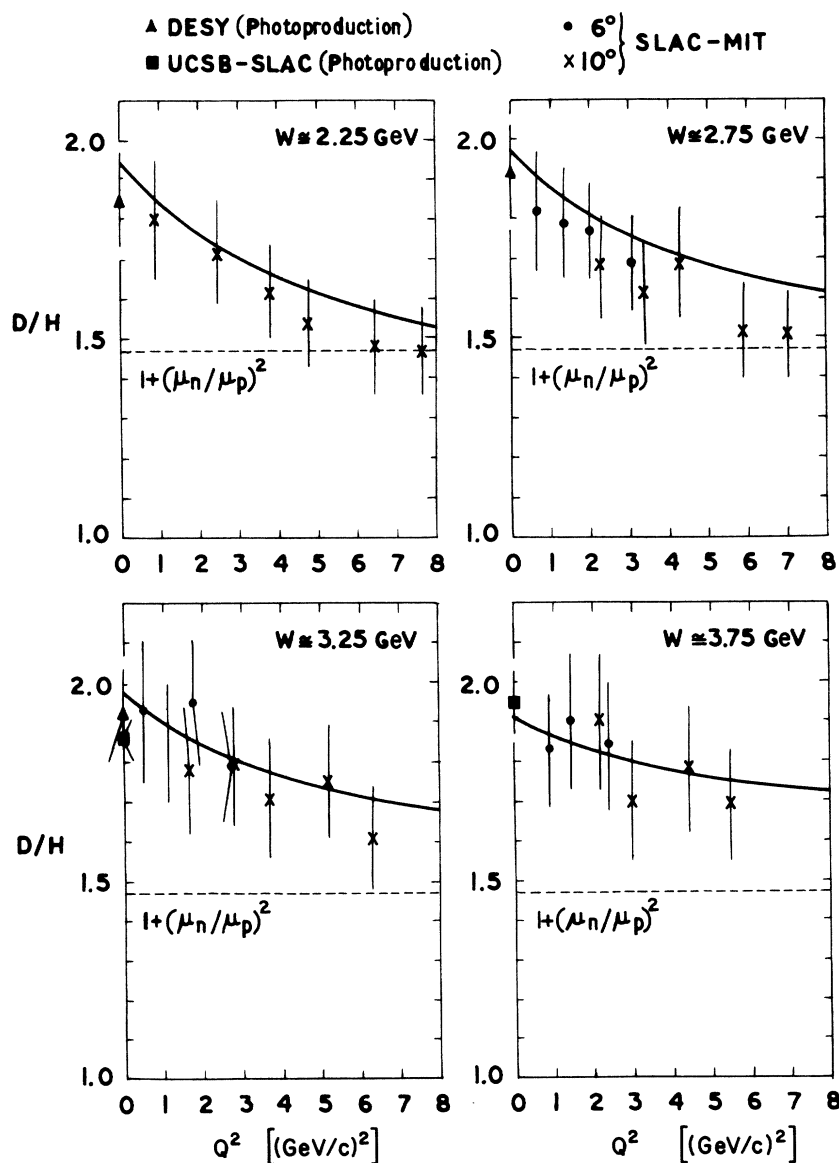


FIG. 9. The quantity  $1 + (\nu W_2^2 / \nu W_1^2) = D/H$  plotted versus  $Q^2$  for different fixed values of  $W$ . The solid curves are our fits. The data are from Bloom *et al.*, Ref. 23, and the dashed line corresponds to the prediction of Ref. 30.

the various contributions [Eqs. (36)–(38)] to the  $p$ - $n$  mass difference have been evaluated by direct numerical integration. The Born contribution is given by

$$\Delta m_{\text{Born}} = \Delta m_B + \Delta m_{\text{sub,poles}},$$

where  $\Delta m_B$  is given by (36) and  $\Delta m_{\text{sub}}$  is the pole contribution of the subtraction term:

$$\Delta m_{\text{sub,poles}} = -\frac{3}{8} \int_0^\infty dQ^2 Q^2 \Delta t_1^{\text{poles}}(-Q^2, 0).$$

The  $Q^2$  integration is rapidly convergent by virtue of the form factors and the results for  $\Delta m_B$  and  $\Delta m_{\text{sub,poles}}$  are found to be

$$\Delta m_B = +1.41 \text{ MeV}$$

and

$$\Delta m_{\text{sub,poles}} = -0.71 \text{ MeV},$$

respectively, leading to

$$\Delta m_{\text{Born}} = -0.70 \text{ MeV}.$$

(66)

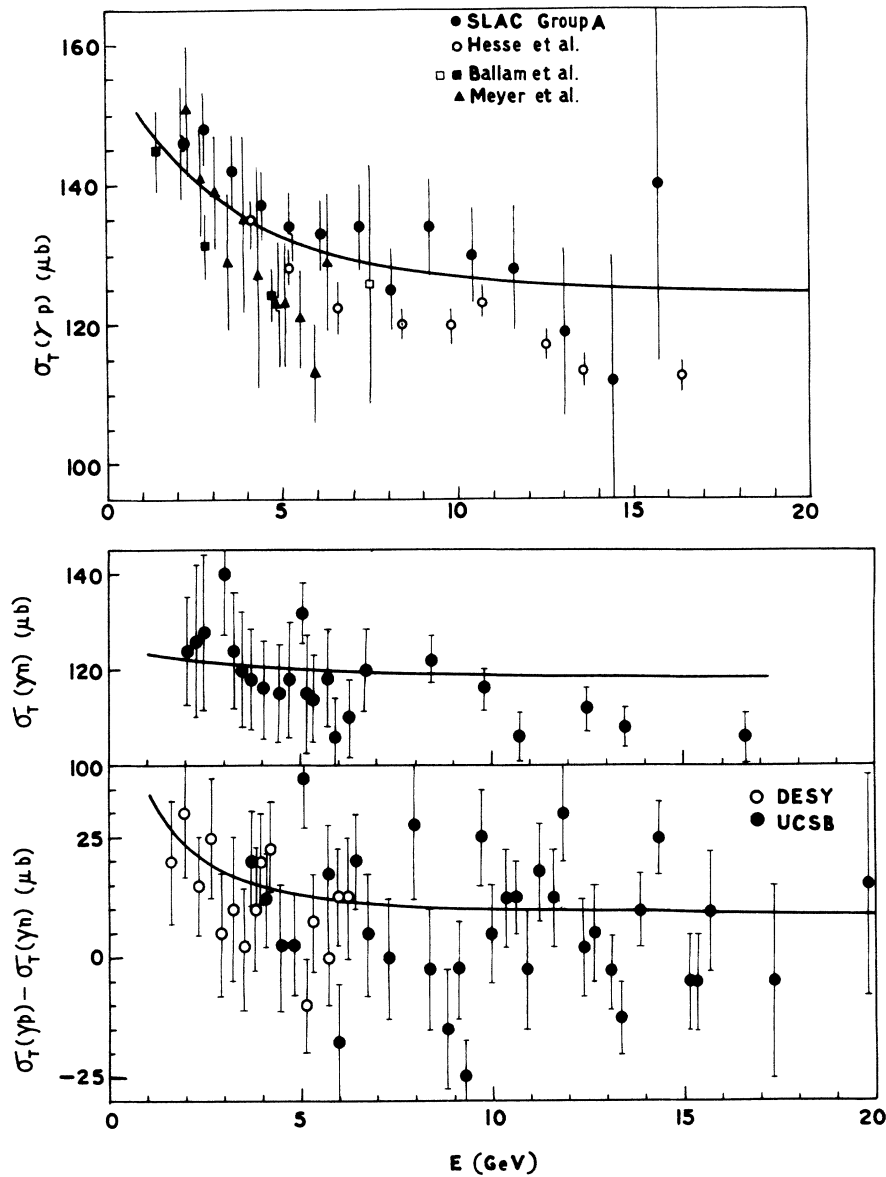


FIG. 10. The photoabsorption cross sections  $\sigma_T(\gamma p)$ ,  $\sigma_T(\gamma n)$  and their difference  $\sigma_T(\gamma p) - \sigma_T(\gamma n)$ , plotted as function of the photon energy  $E$ . The data for the proton and neutron cross sections  $\sigma_T(\gamma p)$ ,  $\sigma_T(\gamma n)$  are from Ref. 32 and those for  $\sigma_T(\gamma p) - \sigma_T(\gamma n)$  are from Ref. 33. The solid lines are our fits.

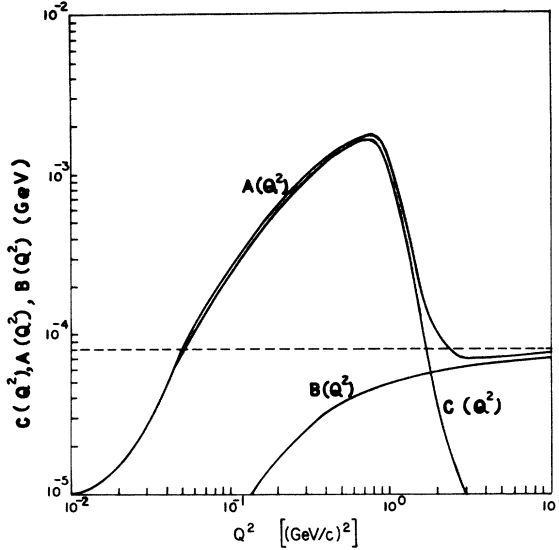


FIG. 11. Illustration of validity of the condition [Eq. (39) of text] for no logarithmic divergence of the Cottingham integral for the mass difference. The dashed line represents the value of

$$\left(\frac{3\alpha m}{8\pi}\right) \int_0^1 dx [\Delta F_2(x) + 2x\Delta F_1(x)],$$

$A(Q^2)$  and  $B(Q^2)$  are the inelastic contributions from the subtraction term and other terms defined [Eq. (67)] such that the mass difference is given by

$$\Delta m = (\Delta m)_{\text{Born}} - \int_0^{\Lambda^2} \frac{dQ^2}{Q^2} [A(Q^2) - B(Q^2)],$$

and  $C(Q^2) \equiv A(Q^2) - B(Q^2)$ .

The inelastic contribution can be represented as

$$\Delta m_{\text{incl}} \equiv \Delta m_{\text{sub}}^I + \Delta m_I = - \int_0^{\Lambda^2} \frac{dQ^2}{Q^2} [A(Q^2) - B(Q^2)], \quad (67)$$

where  $A(Q^2) = \frac{1}{8} Q^4 \Delta F_1^I(-Q^2, 0)$  is the inelastic contribution of the subtraction term.  $B(Q^2)$  is defined by Eq. (37) and represents the remaining inelastic contribution. The  $Q^2$  integration in (67) is also rapidly convergent by virtue of the convergence condition given by Eq. (39). In (67) the major support comes from the region of low  $Q^2$ ,  $Q^2 < \Lambda^2$  where  $\Lambda^2 \approx 3.0$  (GeV)<sup>2</sup> (Fig. 11). The respective contributions from subtraction and other terms from this region are given by

$$\Delta m_{\text{sub}}^I = - \int_0^{\Lambda^2} \frac{dQ^2}{Q^2} A(Q^2) = -2.8 \text{ MeV} \quad (68)$$

and

$$\Delta m_I = \int_0^{\Lambda^2} \frac{dQ^2}{Q^2} B(Q^2) = +0.14 \text{ MeV}, \quad (69)$$

which lead to

$$\Delta m_{\text{incl}} = -2.66 \text{ MeV}. \quad (70)$$

The Born and inelastic contributions as given by (66) and (70) add up to give the final result for the mass difference:

$$\Delta m = -1.96 \pm 0.52 \text{ MeV}. \quad (71)$$

The error quoted in  $\Delta m$  is mostly due to the errors in the parameters, and these errors have been determined to be about 4% of their quoted values.

The above result shows that the subtraction term is mainly responsible for the correct sign and magnitude of the mass difference. This has been made possible by the fact that the inelastic contribution of the subtraction term (which has the right sign) is several orders of magnitude larger (Fig. 11) than the remaining inelastic contribution at finite  $Q^2$ . It cancels asymptotically with the latter, and the net result for the mass difference is rendered finite.

## VI. SUMMARY AND CONCLUSION

We have proposed a model for the forward (virtual) Compton amplitude in very simple form consisting of contributions from Born, inelastic, and subtraction terms. We have ensured manifest analyticity in the  $\nu$  plane,  $s$ - $u$  crossing symmetry, Regge behavior, and Bjorken scale invariance for the amplitudes in appropriate limits as well as the various real photon ( $Q^2 \rightarrow 0$ ) limits. This has been made possible by appealing to the technique of conformal mapping, which exhibits considerable flexibility, making it possible to incorporate in a much more transparent manner all the above properties simultaneously into the theory. In this respect the present model differs significantly from most other scale-invariant Regge-pole and vector-dominance models,<sup>14,15,16</sup> although there exist certain resemblances with these models in some specific kinematical regions, such as the Regge or scale invariance regions. The main results from our model are summarized in the following:

(a) Very good fits to the existing data on electro-production structure functions  $\nu W_2^p$ ,  $2mW_1^p$ ,  $\nu W_2^p - \nu W_2^n$ ,  $\nu W_2^n / \nu W_2^p$ , and  $\nu R_p$  are obtained. The scale-invariance breaking as exhibited by the data on  $\nu W_2^p$  plotted as functions of  $Q^2$  for various fixed values of  $\omega$  as well as the behavior of the quantity  $(1 + \nu W_2^n / \nu W_2^p)$  plotted as a function of  $Q^2$  at various fixed values of  $W^2$  are quite successfully predicted from the model. Further predictions are very good fits to the data on photoabsorption cross sections  $\sigma_T(\gamma p)$ ,  $\sigma_T(\gamma n)$  and  $\sigma_T(\gamma p) - \sigma_T(\gamma n)$  as a function of the photon energy.

(b) We have evaluated the subtraction term

$t_1(-Q^2, 0)$  from a simple ansatz which is consistent with experimental and theoretical considerations.

(c) The principal result of the present model is the parameter-free realization of a finite  $p$ - $n$  mass difference having *correct sign* and right order of magnitude which is quite close to the experimental value. The fact that excellent fits to various available data on electroproduction and photoabsorption have been obtained is significant in itself and lends additional support to the model.

It is not surprising that the subtraction piece plays the most important role in this successful calculation of the mass difference, since the origin and physics of the contributions from other terms, i.e., the Born and deep-inelastic pieces, are understood well in the light of the data on the electromagnetic form factors and the deep-inelastic structure functions of proton and neutron, whereas

the dynamics lying hidden in the subtraction piece has not yet been explored in detail.

The present calculation would lend support to the conjecture put forth by some authors<sup>36</sup> that the inelastic contribution of the subtraction piece transforms as a Coleman-Glashow<sup>35</sup> tadpole in the tadpole model, which successfully accounted in a pure phenomenological way for the mass splittings between the various hadronic isomultiplets.

#### ACKNOWLEDGMENTS

All the calculations and data fittings were performed on an IBM-1130 at the Computer Centre of the Utkal University and we are thankful to the operating staff for their cooperation. One of us (B. P. M.) gratefully acknowledges a junior research fellowship from the University Grants Commission, India, for carrying out this work.

\*Present address: Max-Planck-Institut für Physik und Astrophysik, 8 München—40, Föhringer Ring—6, Postfach-401212, München, West Germany.

<sup>1</sup>For a comprehensive review see A. Zee, Phys. Rep. **3C**, 129 (1972).

<sup>2</sup>R. P. Feynman and G. Speisman, Phys. Rev. **94**, 500 (1954).

<sup>3</sup>M. Cini, E. Ferrari, and R. Gatto, Phys. Rev. Lett. **2**, 7 (1959).

<sup>4</sup>W. N. Cottingham, Ann. Phys. (N. Y.) **25**, 424 (1963).

<sup>5</sup>(a) H. Harari, Phys. Rev. Lett. **17**, 1303 (1966); (b) S. Coleman and H. J. Schnitzer, Phys. Rev. **136**, B223 (1964).

<sup>6</sup>J. D. Bjorken, Phys. Rev. **179**, 1547 (1969).

<sup>7</sup>H. Pagels, Phys. Rev. **185**, 1990 (1969).

<sup>8</sup>J. W. Moffat and A. C. D. Wright, Phys. Rev. D **5**, 75 (1972).

<sup>9</sup>H. Goldberg and Y. N. Srivastava, Phys. Rev. D **4**, 1426 (1971); G. B. West, *ibid.* D **5**, 1987 (1972).

<sup>10</sup>We follow the notations of M. Elitzur and H. Harari, Ann. Phys. (N. Y.) **56**, 81 (1970).

<sup>11</sup>The analyticity of  $t_1(q^2, \nu)$  in both  $\nu$  and  $q^2$  is quite complicated; see A. Suri, Phys. Rev. D **4**, 570 (1971). However, the analyticity in  $\nu$  for fixed  $q^2$  is what concerns us in the present work.

<sup>12</sup>The presence of ( $J=0$ ) fixed poles would modify the right-hand sides of Eqs. (9) and (10) by adding up the residues at these fixed poles:  $R_1(q^2)$  and  $R_2(q^2)$ , respectively (see Ref. 13). We, in the present work, ignore their presence since the nature and origin of these fixed poles are not yet clearly understood.

<sup>13</sup>H. Pagels, Phys. Rev. **172**, 1381 (1968).

<sup>14</sup>J. W. Moffat and V. G. Snell, Phys. Rev. D **3**, 2848 (1971).

<sup>15</sup>B. H. Kellet, Phys. Rev. D **7**, 115 (1973).

<sup>16</sup>J. W. Moffat and A. C. D. Wright, Phys. Rev. D **8**, 2152 (1973).

<sup>17</sup>At this point we observe that the so-called Callan-Gross relation,<sup>18</sup>  $W_1 = (\nu^2/Q^2)W_2$ , i.e.,  $2mW_1 = \omega(\nu W_2)$ , which

has been utilized by several authors (see Refs. 8, 14, and 15), would require  $\text{Im}t_1(-Q^2, \nu) \rightarrow 0$  in the Regge limit ( $\nu \rightarrow \infty$ ,  $Q^2$  fixed). But this would then imply that  $t_1$ , as well, satisfies an unsubtracted dispersion relation in  $\nu$  for fixed  $Q^2$ , in contradiction to Harari's (see Ref. 5) analysis. The relation further implies a functional form of  $R$ :  $R = Q^2/\nu^2$ . Although the present data (see Ref. 34) on  $R$  do not rule out this possibility, they seem to have a definite tendency against such behavior [Also see in this connection J. J. Sakurai, Phys. Rev. Lett. **30**, 245 (1973)]. The above consideration plays a crucial role in the evaluation of the subtraction term in  $t_1$  and hence in the calculation of the  $p$ - $n$  mass difference.

<sup>18</sup>C. G. Callan and D. J. Gross, Phys. Rev. Lett. **22**, 156 (1969).

<sup>19</sup>For a critical examination of the criteria for this Wick rotation, see Elitzur and Harari, Ref. 10.

<sup>20</sup>S. D. Drell and T.-M. Yan, Phys. Rev. Lett. **24**, 181 (1970); G. B. West, *ibid.* **24**, 1206 (1970).

<sup>21</sup> $l_p, l_n$ , and  $k$  are constrained to integral values on ground of analyticity of the amplitudes  $t_1^N$ .

<sup>22</sup>A. Bodek *et al.*, Phys. Rev. Lett. **30**, 1087 (1973).

<sup>23</sup>G. Miller *et al.*, Phys. Rev. D **5**, 528 (1972); E. D. Bloom *et al.*, SLAC Report No. SLAC-PUB-796, 1970 (unpublished), presented at the XV International Conference on High Energy Physics, Kiev, U. S. S. R.

<sup>24</sup>That we have chosen  $\omega$  (and not any other variable, such as  $\omega'$ ) as the scaling variable to work with, is due to the fact that, for fixed  $Q^2$ ,  $\omega$  is proportional to  $\nu$  such that the analytic structures of the amplitudes  $t_1^N$  are similar in nature in both  $\nu$  and  $\omega$  planes, and, therefore, the same mapped variable  $Z$  describes both  $\nu$ - and  $\omega$ -plane analyticity at fixed  $Q^2$ .

<sup>25</sup> $\chi^2$  has the usual definition,

$$\chi^2 = (1/n) \sum_{i=1}^n \{[\text{Th. (i)} - \text{Expt. (i)}] / \text{Er (i)}\}^2,$$

where  $n$  is the number of data points and other terms have their usual meaning.

- <sup>26</sup>See in this connection H. K. Shepard and L. M. Simmons, Jr., Phys. Rev. D 8, 2114 (1973) and references cited therein [particularly the paper by Landshoff and Polkinghorne, Nucl. Phys. B52, 473 (1973)].
- <sup>27</sup>S. D. Drell, D. Levy, and T.-M. Yan, Phys. Rev. 187, 2159 (1969); Phys. Rev. D 1, 1617 (1970).
- <sup>28</sup>H. Harari, Phys. Rev. Lett. 22, 1078 (1969); 24, 286 (1970).
- <sup>29</sup>F. E. Close and J. F. Gunion, Phys. Rev. D 4, 742 (1971); 4, 1576 (1971).
- <sup>30</sup>E. D. Bloom and F. J. Gilman, Phys. Rev. Lett. 25, 1140 (1970); Phys. Rev. D 4, 2901 (1971).
- <sup>31</sup>O. Nachtmann, Phys. Rev. D 5, 686 (1972).
- <sup>32</sup>D. O. Caldwell *et al.*, Phys. Rev. Lett. 23, 1256 (1969); 25, 609 (1970); W. P. Hesse *et al.*, *ibid.* 25, 613 (1970); H. Meyer *et al.*, Phys. Lett. 33B, 189 (1970); J. Ballam *et al.*, Phys. Rev. Lett. 23, 498 (1969); E. D. Bloom *et al.*, SLAC Report No. SLAC-PUB-653, 1969 (unpublished).
- <sup>33</sup>*Proceedings of the International Symposium on Electron and Photon Interactions at High Energy, 1971*, edited by N. B. Mistry (Laboratory of Nuclear Studies, Cornell Univ., Ithaca, N. Y., 1972).
- <sup>34</sup>E. M. Riordan *et al.*, Phys. Rev. Lett. 33, 561 (1974).
- <sup>35</sup>S. Coleman and S. L. Glashow, Phys. Rev. 134, B671 (1964).
- <sup>36</sup>S. Okubo, Phys. Rev. Lett. 18, 256 (1967); Y. Liu and S. Okubo, Nuovo Cimento 52, 1186 (1967).